TECHNICAL REPORT R-33

DESIGN OF AXISYMMETRIC EXHAUST NOZZLES BY METHOD OF CHARACTERISTICS INCORPORATING A VARIABLE ISENTROPIC EXPONENT

By ELEANOR COSTILOW GUENTERT and HARVEY E. NEUMANN

Lewis Research Center
Cleveland, Ohio

TECHNICAL REPORT R-33

DESIGN OF AXISYMMETRIC EXHAUST NOZZLES BY METHOD OF CHARACTERISTICS INCORPORATING A VARIABLE ISENTROPIC EXPONENT

By Eleanor Costilow Guentert and Harvey E. Neumann

SUMMARY

An analytical method for including a variable isentropic exponent in the method of characteristics as applied to the design of rocket nozzles has been obtained, which is independent of the manner in which the initial boundary conditions are specified for the problem. The method incorporates existing thermodynamic data for either frozen or equilibrium composition in the characteristic flow equations of supersonic flow.

The design of several nozzles was attempted by specification of the initial boundary conditions along the nozzle centerline. It was extremely difficult, however, to specify the flow distribution along the nozzle axis and to obtain solutions to the characteristic equations yielding short-length nozzles. Selection of adequate initial boundary conditions appears to be a trial-and-error process based upon previous experience. For the case where nozzle length is not important, designs are readily obtainable by utilizing a geometric scaling procedure. Several bell-shaped nozzles have been designed by specifying the initial boundary conditions along the nozzle centerline and by utilizing geometric scaling.

A comparison is presented of nozzle contours obtained by assuming either frozen or equilibrium composition. A comparison of contours for both compositions with either constant or variable isentropic exponent is also presented. Ammonia-oxygen was used as the propellant combination in the comparison. Significant differences among the contours of the examples indicated that the assumption of constant isentropic exponent is inadequate and that actual thermodynamic data should be used in the solution of the characteristic flow equations.

A computation of the variation of vacuum specific impulse with axial length showed that considerable nozzle length, and hence weight, can be eliminated without serious thrust penalties in nozzle designs that gradually expand the flow to uniform exit conditions. For the example computed, a reduction in axial length of 50 percent resulted in only a 1.6-percent reduction in vacuum specific impulse.

INTRODUCTION

Generally, the technique described for shock-free nozzle design is the method of characteristics, which is a linearized solution of the supersonic flow equations. Previous application of the method of characteristics to nozzle design has considered the isentropic exponent γ to be constant throughout the expansion process. (All symbols are defined in appendix A.) Reference 1 presents a rocket-nozzle design using the method of characteristics where the isentropic exponent is held constant.

The nature of the expansion process in a nozzle is dependent on the chemical kinetics of the gas species. Unfortunately, little information exists on the chemical kinetics as applied to a rocket nozzle, and hence an exact determination of the expansion process is impossible. Thermodynamic data do exist, however, for the two limiting expansion processes where the reaction rates are considered to be either infinitely slow or infinitely fast. For these two processes, the chemical composition remains either constant (frozen) or in equilibrium throughout the expansion.

A comparison of one-dimensional isentropic-expansion computations for the frozen and equilibrium cases shows that there is a considerable difference in the area-ratio requirement for a given expansion pressure ratio. Also, for both equilibrium and frozen expansion, γ does not remain constant throughout the expansion process. Consequently, in computing the contours of nozzles for high-temperature gases, the method of characteristics should include γ as a variable.

This report contains a description of the analytical method for including γ as a variable in the method of characteristics. The analytical method uses existing thermodynamic data for frozen or equilibrium composition and incorporates these data in the characteristic equations of supersonic flow. The method for including variable γ is not dependent on the manner in which the initial boundary conditions are specified for the problem.

Included in this report are several bell-shaped nozzles that have been designed by the method of characteristics for use with the stoichiometric combustion products of ammonia and oxygen. These nozzles were designed for use in a rocket-powered supersonic tunnel described in reference 2.

A comparison is presented of the nozzle contours obtained by using frozen or equilibrium composition. A comparison of contours is also presented for both compositions with both constant and variable isentropic exponent. Also included in the nozzle-design technique is a computational method for determining the specific impulse at each axial station along the nozzle axis. This type of computation is particularly applicable to studies of rocket nozzles where information on the relation between thrust and length is important. From the nozzle designs presented herein, some idea of the thrust penalties incurred because of shortening the length of a characteristic nozzle can be obtained.

METHOD OF ANALYSIS

AXISYMMETRIC POTENTIAL-FLOW CHARACTERISTIC EQUATIONS

The axisymmetric characteristic equations for steady, irrotational, isentropic flow used in this analysis were those presented by A. Ferri in reference 3. The characteristic equations are obtained by combining the equations of motion and continuity. Another relation is derived from the geometric properties of the characteristic line. The resulting equations for the two characteristic lines associated with each point in the flow field are

First family:

$$\left\{\begin{aligned} &\left(\frac{dy}{dx}\right)_1=\tan(\theta+\mu) &(1)\\ &\frac{dV}{V}-\tan\mu\,d\theta-\frac{\tan\mu\sin\mu\sin\theta}{\cos(\theta+\mu)}\frac{dx}{y}=0 &(2)\end{aligned}\right.$$

and, second family:

$$\left\{\begin{aligned} &\left(\frac{dy}{dx}\right)_2=\tan(\theta-\mu) &(3)\\ &\frac{dV}{V}+\tan\mu\,d\theta-\frac{\tan\mu\sin\mu\sin\theta}{\cos(\theta-\mu)}\frac{dx}{y}=0 &(4)\end{aligned}\right.$$

The Mach angle μ in equations (1) to (4) is dependent on γ and is therefore a variable at every point in the flow field. In figure 1 the velocity

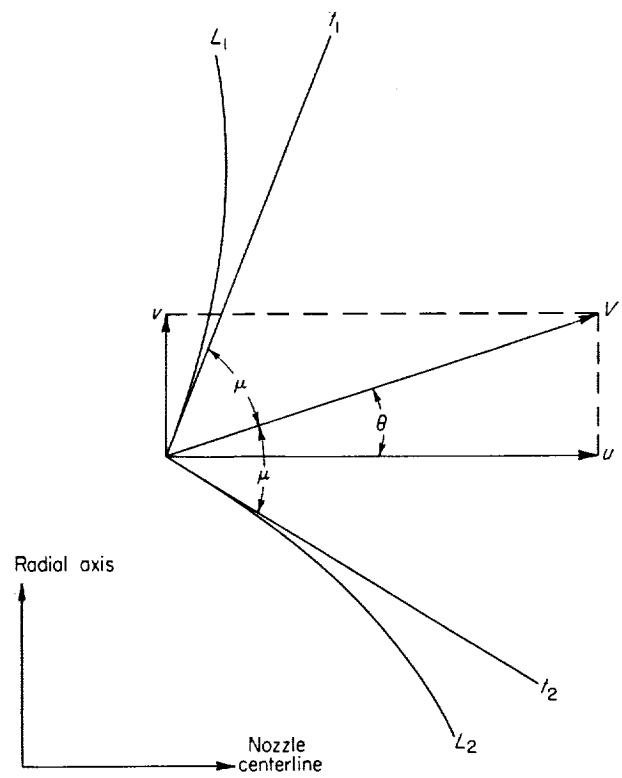

FIGURE 1.—Characteristic lines and velocity vectors for a general point in the supersonic stream.

component and angle relations are given for a characteristic point in the supersonic flow field. The same notation used by A. Ferri in reference 3 has been followed.

FINITE-DIFFERENCE SOLUTION OF CHARACTERISTIC EQUATIONS

Equations (1) to (4) are numerically integrated by rewriting the differential equations in the form of finite differences and following a point-to-point calculation of the flow properties throughout the flow field. Figure 2 shows two points, A and B,

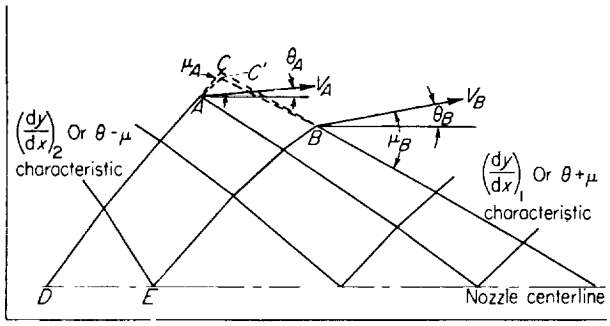

FIGURE 2.—Point calculation system in the characteristic network.

in the characteristic network, whose properties are known. If the distance between characteristic points is kept small, the tangents of the characteristics can be assumed to represent the characteristics themselves for a first approximation. The tangents of the characteristics from two different families at points B and A, that is, $\tan(\theta_B-\mu_B)$ and $\tan(\theta_A+\mu_A)$, respectively, intersect at point C. The flow properties and location at C are determined by first solving equations (1) and (3) simultaneously for x_C and y_C; and second, knowing x_C and y_C, equations (2) and (4) are solved simultaneously for V_C and θ_C. Thus for the first approximation, the location of point C is given by equations (1) and (3) in finite-difference form:

$$\frac{y_C-y_A}{x_C-x_A}=\tan(\theta_A+\mu_A) \tag{5}$$

$$\frac{y_C-y_B}{x_C-x_B}=\tan(\theta_B-\mu_B) \tag{6}$$

Solving for x_C from equations (5) and (6) yields

$$x_C=\frac{y_A-y_B+x_B\tan(\theta_B-\mu_B)-x_A\tan(\theta_A+\mu_A)}{\tan(\theta_B-\mu_B)-\tan(\theta_A+\mu_A)} \tag{7}$$

and for y_C,

$$y_C=y_A+(x_C-x_A)\tan(\theta_A+\mu_A) \tag{8}$$

Likewise, finite-difference equations can replace the differential equations (2) and (4), so that they become

$$\frac{V_C-V_A}{V_A}-(\theta_C-\theta_A)\tan\mu_A-\frac{\tan\mu_A\sin\mu_A\sin\theta_A}{\cos(\theta_A+\mu_A)}\frac{(x_C-x_A)}{y_A}=0 \tag{9}$$

and

$$\frac{V_C-V_B}{V_B}+(\theta_C-\theta_B)\tan\mu_B-\frac{\tan\mu_B\sin\mu_B\sin\theta_B}{\cos(\theta_B-\mu_B)}\frac{(x_C-x_B)}{y_B}=0 \tag{10}$$

By solving for V_C by elimination of θ_C, the following relation is obtained:

$$V_C=\frac{1}{\frac{\cot\mu_A}{V_A}+\frac{\cot\mu_B}{V_B}}\{\cot\mu_A[1+\mathscr{L}_A(x_C-x_A)]+\cot\mu_B[1+\mathscr{M}_B(x_C-x_B)]+\theta_B-\theta_A\} \tag{11}$$

where

$$\mathscr{L}_A=\frac{\tan\mu_A\sin\mu_A\sin\theta_A}{y_A\cos(\theta_A+\mu_A)}$$

$$\mathscr{M}_B=\frac{\tan\mu_B\sin\mu_B\sin\theta_B}{y_B\cos(\theta_B-\mu_B)}$$

and solving for the flow angle θ_C, the following relation is obtained:

$$\theta_C=\theta_A+\cot\mu_A\left[\frac{V_C-V_A}{V_A}-\mathscr{L}_A(x_C-x_A)\right] \tag{12}$$

The values obtained from equations (7), (8), (11), and (12) are only a first approximation, since all the coefficients in the equations were based on the properties at points A and B. Usually a second iteration of the equation is required where the coefficients of the differential equations are averaged between A and C, and B and C. Thus, the second iteration point is located at C', and equations (7) and (8) become

$$x_{C'}=\frac{y_A-y_B+\frac{1}{2}[\tan(\theta_B-\mu_B)+\tan(\theta_C-\mu_C)]x_B-\frac{1}{2}[\tan(\theta_A+\mu_A)+\tan(\theta_C+\mu_C)]x_A}{\frac{1}{2}[\tan(\theta_B-\mu_B)+\tan(\theta_C-\mu_C)-\tan(\theta_A+\mu_A)-\tan(\theta_C+\mu_C)]}$$

and

$$y_{C'}=y_A+(x_C-x_A)\frac{1}{2}[\tan(\theta_A+\mu_A)+\tan(\theta_C+\mu_C)]$$

Similarly, equations (11) and (12) become

$$V_{C'}=\frac{1}{4[(V_A+V_C)^{-1}(\tan\mu_A+\tan\mu_C)^{-1}+(V_B+V_C)^{-1}(\tan\mu_B+\tan\mu_C)^{-1}]}$$

$$\left\{\frac{2}{\tan\mu_A+\tan\mu_C}\left[\frac{2V_A}{V_A+V_C}+\frac{\mathscr{L}_A+\mathscr{L}_C}{2}(x_C-x_A)\right]\right.$$

$$\left.+\frac{2}{\tan\mu_B+\tan\mu_C}\left[\frac{2V_B}{V_B+V_C}+\frac{\mathscr{M}_B+\mathscr{M}_C}{2}(x_C-x_B)\right]+\theta_B-\theta_A\right\}$$

and

$$\theta_{C'}=\theta_A+\frac{2}{\tan\mu_A+\tan\mu_C}\left[\frac{2(V_C'-V_A)}{V_C+V_A}-\frac{\mathscr{L}_A+\mathscr{L}_C}{2}(x_C-x_A)\right]$$

Apparently, in order to iterate the equations after the first approximation, the value of Mach angle μ at C must be obtained so that the coefficients can be averaged. In order to calculate the Mach angle at C, the speed of sound must be determined from the thermodynamic properties of the gas. If the properties change significantly between the first and second iterations, a third iteration may be required. After the flow properties at C' have been determined within the desired accuracy, point C' becomes a starting point for the calculation of future points of the network.

THERMODYNAMIC ANALYSIS

The isentropic exponent is an important parameter in all compressible-flow processes but can be considered to be constant in any low-temperature airflow analysis. However, in a rocket nozzle operating with high-pressure and high-temperature gases, the dissociation effects of the gas should be included in the supersonic characteristic flow solutions. The dissociation and reassociation phenomena and chemical kinetics cause the molecular weight of the combustion gases to vary with both time and position in the nozzle. When the molecular weight varies, the isentropic exponent (which enters into the computation of the speed of sound) cannot be expressed as the ratio of specific heats, but must include a function of the rate of change of molecular weight with pressure. The expression for the insentropic exponent can easily be derived from its definition by using the tables of reference 4 and the equation of state. Hence,

$$\gamma=\frac{c_p}{c_v}\left[1+\left(\frac{\partial\ln m}{\partial\ln p}\right)_T\right]^{-1} \tag{13}$$

The relation between molecular weight and pressure for evaluation of the isentropic exponent is dependent on the chemical kinetics of the chemical constituents of the reacting combustion gas. Unfortunately, the necessary chemical kinetics are not known for current rocket propellants except for the two limiting cases of frozen and equilibrium composition. A generalized method for computing the thermodynamic properties of a combustion gas assuming equilibrium or frozen composition is given in reference 5, and data for a number of rocket propellant combinations are presented in references 6 to 10.

The data for frozen or equilibrium composition can be incorporated into the finite-difference solution of the characteristic equations by utilizing the appropriate thermodynamic relations. Inserting the thermodynamic data into the characteristics solution can be achieved with only minor additions to the method of characteristics. When high-speed automatic-computing machines are utilized to obtain a characteristic solution, adding the thermodynamic data to the solution of the method of characteristics does not add undue complications.

Any thermodynamic property can always be considered to be only a function of any two other thermodynamic properties. For an isentropic

process it is therefore possible to express all thermodynamic data for a given entropy level in terms of only one thermodynamic property. If the enthalpy is considered to be some function φ of the natural logarithm of the pressure, then from the energy equation for isentropic flow the static-temperature molecular-weight ratio can be obtained from

$$R\frac{T}{m}=\frac{\mathrm{d}H}{\mathrm{d}\ln p}=\frac{\mathrm{d}\varphi}{\mathrm{d}\ln p} \tag{14}$$

Similarly, the following γ function can be obtained by using the tables of reference 4 and the equation of state:

$$\frac{\gamma-1}{\gamma}=\frac{\mathrm{d}\ln\frac{T}{m}}{\mathrm{d}\ln p}=\frac{\mathrm{d}^2\varphi}{\mathrm{d}(\ln p)^2}\Big/\frac{\mathrm{d}\varphi}{\mathrm{d}(\ln p)} \tag{15}$$

Equation (15) gives the isentropic exponent based on the thermodynamic properties of the rocket gases for each point in the nozzle. If the local-temperature molecular-weight ratio and the local isentropic exponent are known, the speed of sound at the point in the flow is determined from

$$a=\left(\frac{\gamma gRT}{m}\right)^{1/2} \tag{16}$$

The thermodynamic properties are related to the velocity by the energy equation in the form

$$V=K_q(H_c-H)^{1/2}=K_q(H_c-\varphi)^{1/2} \tag{17}$$

Equations (14) to (17) give the relations necessary to evaluate the Mach angle μ for any given velocity.

The enthalpy function φ was obtained by fitting the data for frozen or equilibrium composition over the pressure range for the nozzle design. The following numerical relation using $\ln p$ as a parameter was fitted to the thermodynamic data:

$$\varphi\equiv H=K_1+K_2(\ln p)+K_3(\ln p)^2+K_4(\ln p)^3+K_5(\ln p)^4+K_6(\ln p)^5 \tag{18}$$

The preceding method for including variable γ in the method of characteristics is general and is independent of the manner in which the initial boundary conditions are specified for the problem.

APPLICATION OF THE CHARACTERISTIC EQUATIONS

The method for incorporating the thermodynamic data into the characteristic equations was used to design a shock-free divergent section for the ammonia-oxygen rocket tunnel with a chamber pressure of 600 pounds per square inch reported in reference 2. For design of nozzles for tunnel application it is necessary to specify the exit flow and then determine the contour that will produce that flow. A weight flow of 19.06 pounds per second and an exit pressure of approximately 1.7 pounds per square inch absolute were desired for operation at stoichiometric conditions. This corresponds to an exit Mach number of approximately 4.0. The thermodynamic data incorporated in the characteristic calculations are reported in reference 10. The pressure distribution along the nozzle centerline from throat to nozzle exit was prescribed, and the corresponding properties of the gas were determined from equations (14) to (18). (The flow angle along the centerline of an axisymmetric nozzle is zero.) Thus, the properties at any two adjacent points along the centerline of the characteristic network, such as D and E of figure 2, provide the initial information for the solution of the characteristic equations (5), (6), (11), and (12). The finite-difference computation proceeds outward from the nozzle centerline. The details of the computational procedure are given in appendix B.

Solutions to the characteristic equations were obtained for centerline pressure distributions defined as cosine, parabolic, and cubic functions of the axial length. The functions, shown in figure 3, were defined by

Cosine: $$\ln p=\frac{1}{2}(\ln p_t-\ln p_e)\cos\frac{\pi x}{l}+\frac{1}{2}(\ln p_t+\ln p_e) \tag{19}$$

Parabolic: $$\ln p=l^{-2}(x-l)^2(\ln p_t-\ln p_e)+\ln p_e \tag{20}$$

Cubic: $$\ln p=\left[\frac{ql+2(\ln p_t-\ln p_e)}{l^3}\right]x^3-\left[\frac{2ql+3(\ln p_t-\ln p_e)}{l^2}\right]x^2+qx+\ln p_t \tag{21}$$

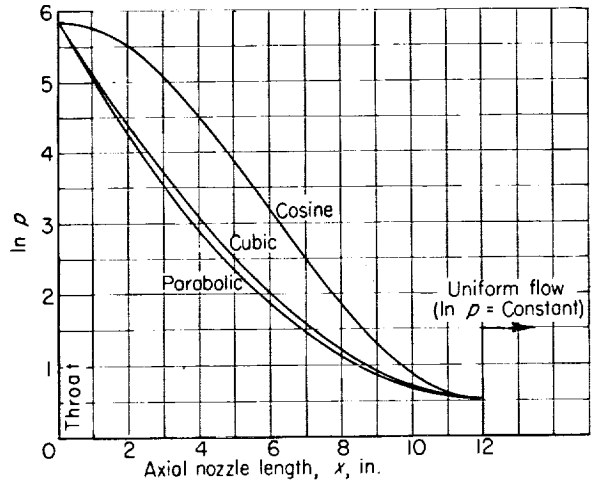

FIGURE 3.—Centerline pressure input distributions.

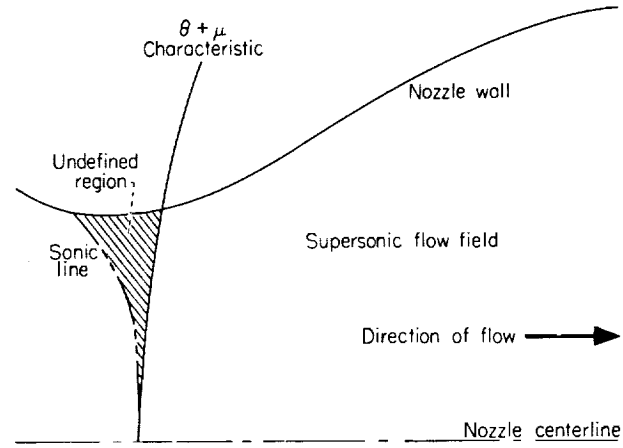

FIGURE 4. Sketch of undefined region of the characteristic solution with boundary conditions specified along nozzle centerline.

The expansion length l chosen was 12 inches, and the exit pressure was 1.7 pounds per square inch absolute. The pressure at the throat was chosen as the value obtained by using equilibrium composition. The coefficients of equations (19) to (21) were determined from the following assumed boundary conditions:

$$\text{at } x=x_t=0, \qquad \mathrm{d}\ln p/\mathrm{d}x=\mathrm{q}, \qquad p=p_t$$

$$\text{at } x=l=12, \qquad \mathrm{d}\ln p/\mathrm{d}x=0, \qquad p=p_e$$

In addition to varying the centerline pressure distribution using equilibrium composition, a comparison was made of the effect of frozen and equilibrium composition upon the solution with a fixed centerline pressure distribution. A comparison was also made (for each composition) of the effects of both fixed and variable isentropic exponent upon the solution when using a fixed centerline pressure distribution.

THROAT CONDITIONS

An initial value problem is defined when the centerline pressure distribution for the supersonic portion of the nozzle is specified. The solution of this initial value problem does not encompass the entire supersonic portion of the nozzle, as shown in figure 4. No solution is obtained for the region between the sonic line and the $\theta+\mu$ characteristic that passes through the sonic point on the centerline. For the case where the throat curvature is very small, the undefined region of the supersonic flow field becomes small, and the flow in this region may be neglected. This is the case for the nozzle designed for the rocket tunnel of reference 2.

ADDITIONAL CALCULATIONS

Weight flow.—Any streamline determined from the results of the characteristic solution generates a shock-free rocket-nozzle contour. A weight-flow computation was carried along with the characteristic calculations so that the data are available for streamline calculations. For instance, consider the weight flow across the characteristic line AC of figure 2:

$$w_C-w_A=\int_A^C (\rho u 2\pi y\,\mathrm{d}y-2\pi\rho v y\,\mathrm{d}x)$$

which reduces to

$$w_C-w_A=2\pi\int_A^C \rho V\left[\cos\theta-\frac{\sin\theta}{\tan(\theta+\mu)}\right]y\,\mathrm{d}y \qquad (22)$$

A numerical integration of equation (22) between characteristic points gives a weight-flow history of the characteristic network, and the streamlines are easily obtained by interpolation.

Vacuum specific impulse.—The vacuum-specific-impulse (assuming the flow discharges to a vacuum) calculation can be executed as the characteristic flow network is being developed. This computation is of considerable importance when the contours of rocket nozzles are being computed because it indicates the effect of nozzle size on thrust. For these calculations the following equa-

tion was used along the family of AC characteristics:

$$I_C=\frac{1}{w_C}\left[F_A+\left(\frac{w_C-w_A}{g}\right)\left(\frac{V_A\cos\theta_A+V_C\cos\theta_C}{2}\right)+\pi\left(\frac{p_A+p_C}{2}\right)(y_C^2-y_A^2)\right] \quad (23)$$

where all values of I, w, and F are integrated values from the centerline to the point represented by the subscript.

RESULTS AND DISCUSSION

The characteristic calculation using equilibrium-composition data with the cosine-function pressure distribution as input showed a coalescing of one family of characteristic lines a short distance downstream of the throat at a weight flow of about 2 pounds per second. This coalescing indicates that it is impossible to obtain a solution having the desired flow rate for this particular centerline pressure distribution.

To learn the effects on the characteristic network of changing the centerline pressure distribution, the parabolic and cubic inputs of figure 3 were also tried. The results were essentially the same as experienced with the cosine input; namely, a coalescing of one of the families of characteristic lines at a weight flow of approximately 2 pounds per second. Thus, it appears that, if the flow-expansion length is too short, it will be extremely difficult to find a characteristic solution with a pressure distribution along the centerline being described by any function of the family of the simple functional relations considered herein. Reference 11 gives a somewhat detailed discussion of the selection of centerline pressure distributions for the related two-dimensional case and points out this problem of coalescing of characteristics. It is indicated that only a trial-and-error method based on previous experience can give the desired characteristic solution. Although no solution was attainable with the inputs of equations (19) to (21), it was possible to scale the solution using the parabolic input to obtain a shock-free contour for the rocket-tunnel weight-flow requirements.

SCALING

Examination of equations (1) to (4) shows that all the coordinates x and y appear only as ratios. It is therefore feasible to use a geometric scaling procedure to obtain nozzle contours with weight flows different from those of existing solutions of the characteristic equations. Since the radial dimension of the nozzle is proportional to the square root of the weight flow, the axial dimension must also vary as the square root of the weight flow in order to preserve geometric similarity. For the streamline with a weight flow of 2.1 pounds per second obtained with the parabolic centerline pressure distribution, a scaling factor of 3 was necessary to scale to a nozzle contour with a weight flow of 19 pounds per second.

The centerline pressure distribution is altered when geometric scaling is used to obtain a new solution. When a 2.1-pound-per-second weight-flow streamline is scaled up to the nozzle with a 19-pound-per-second weight-flow rate, the pressure gradient along the centerline is reduced by a factor of 3. The scaled parabolic centerline pressure distribution is shown in figure 5.

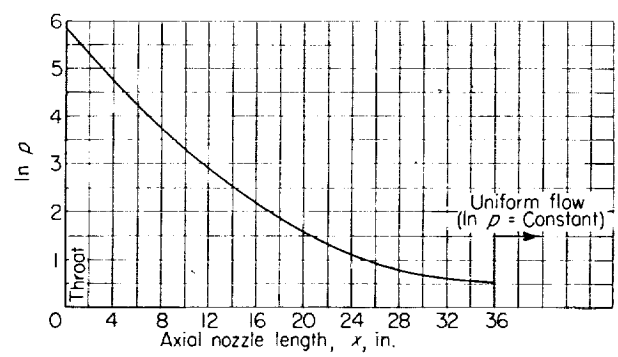

FIGURE 5. Parabolic pressure input scaled three times.

Nozzle designs based upon equilibrium and frozen composition with both variable and constant isentropic exponent for each composition. — The thermodynamic properties of the high-temperature combustion gases in a nozzle are usually somewhere between the extremes determined by assuming equilibrium or frozen composition. The effect of real thermodynamic data on nozzle design can be indicated, however, by examining the effects of the assumption of either frozen or equilibrium composition. The effects of considering a constant γ can be examined by comparison with solutions with variable γ.

The streamlines resulting from the characteristic calculations using the input of figure 5 are

shown in figure 6. The flows obtained by assuming a variable γ and either frozen or equilibrium composition are presented. Also shown in figure 6 are the isobars and streamlines for both frozen and equilibrium composition when the isentropic exponent is held constant. The isentropic exponents used in the two constant γ solutions were the values corresponding to each chamber condition. A value of 1.1402 was used for the isentropic exponent when equilibrium composition was used, while a value of 1.2054 was used with the frozen composition. All other thermodynamic properties used in the two constant γ solutions were identical with those used in the corresponding variable γ solutions.

As shown in the four examples of figure 6, the major portions of the axial length are spent in turning the flow very slowly to the axial direction. This is typical of nozzles designed for tunnel application where gradual accelerations and uniform exit flow are desired.

A comparison of the 4- and 18-pound-per-second streamlines for frozen and equilibrium composition with both fixed and variable γ for each composition is given in figure 7. There is a significant difference in the flow contours for the two variable γ solutions. For the examples computed, the solution with equilibrium composition gives an area in the axial-flow section approximately 20 percent greater than the solution with frozen composition. For frozen composition, the streamlines obtained by assuming a constant γ closely approximate the streamlines obtained by using a variable γ. A slightly larger area ratio results from the constant-isentropic-exponent solution in the middle portion of the nozzle; however, the exit areas are nearly equivalent.

The solution based on constant isentropic exponent with equilibrium composition is significantly different from the other three solutions. The characteristics of the solution with equilibrium composition and a constant γ coalesce at a weight flow of approximately 12 pounds per second, and hence no solution is possible for greater weight flows. Appreciable differences in the streamlines at lower flows are noted. At a weight flow of 4 pounds per second, the differences in streamline shape in the middle portion of the contour between the two equilibrium-composition cases are as great as the differences between the two variable γ cases.

The differences among the solutions based on the different assumptions show that the variation of γ is an important factor in the design of nozzles operating at high temperatures. For more-reactive propellant combinations, such as hydrogen-fluorine, there is an increase in the difference in area-ratio requirements for frozen and equilibrium composition. In addition, the variation of γ between throat conditions and nozzle exit conditions increases for both frozen and equilibrium composition. These effects can be seen by comparing the one-dimensional isentropic data of references 6 to 10. For more-reactive propellant combinations it would therefore become more important to include thermodynamic data that comprehend the effect of a variable isentropic exponent.

Vacuum specific impulse.—The variation of vacuum specific impulse with axial length is of great interest in the design of rocket nozzles. The results of the computation of vacuum specific impulse for the solution obtained with constant γ and equilibrium composition are given in figure 8 for the 4-pound-per-second streamline. Considerable nozzle length, and hence weight, can be eliminated without serious thrust penalties. If the axial length of the 4-pound-per-second streamline is reduced by 50 percent, there is only a 1.6-percent loss in vacuum specific impulse. As the length is further reduced, the loss in vacuum specific impulse increases rapidly. A reduction in length of 75 percent will give a 9.7-percent reduction in vacuum specific impulse. It is hence practical to eliminate a large portion of the nozzle that has the greatest surface area per unit axial length and thus greatly reduce the weight without serious penalties in vacuum specific impulse.

SUMMARY OF RESULTS

An analytical method for including a variable γ in the method of characteristics as applied to the design of rocket nozzles has been obtained. The method of including a variable γ is independent of the manner in which the initial boundary conditions are specified for the problem. The method incorporates existing thermodynamic data for either frozen or equilibrium composition in the characteristic flow equations of supersonic flow.

The design of several nozzles was attempted by specification of the initial boundary conditions along the nozzle centerline. It was extremely difficult, however, to specify the flow distribution along the nozzle axis and to obtain solutions to the

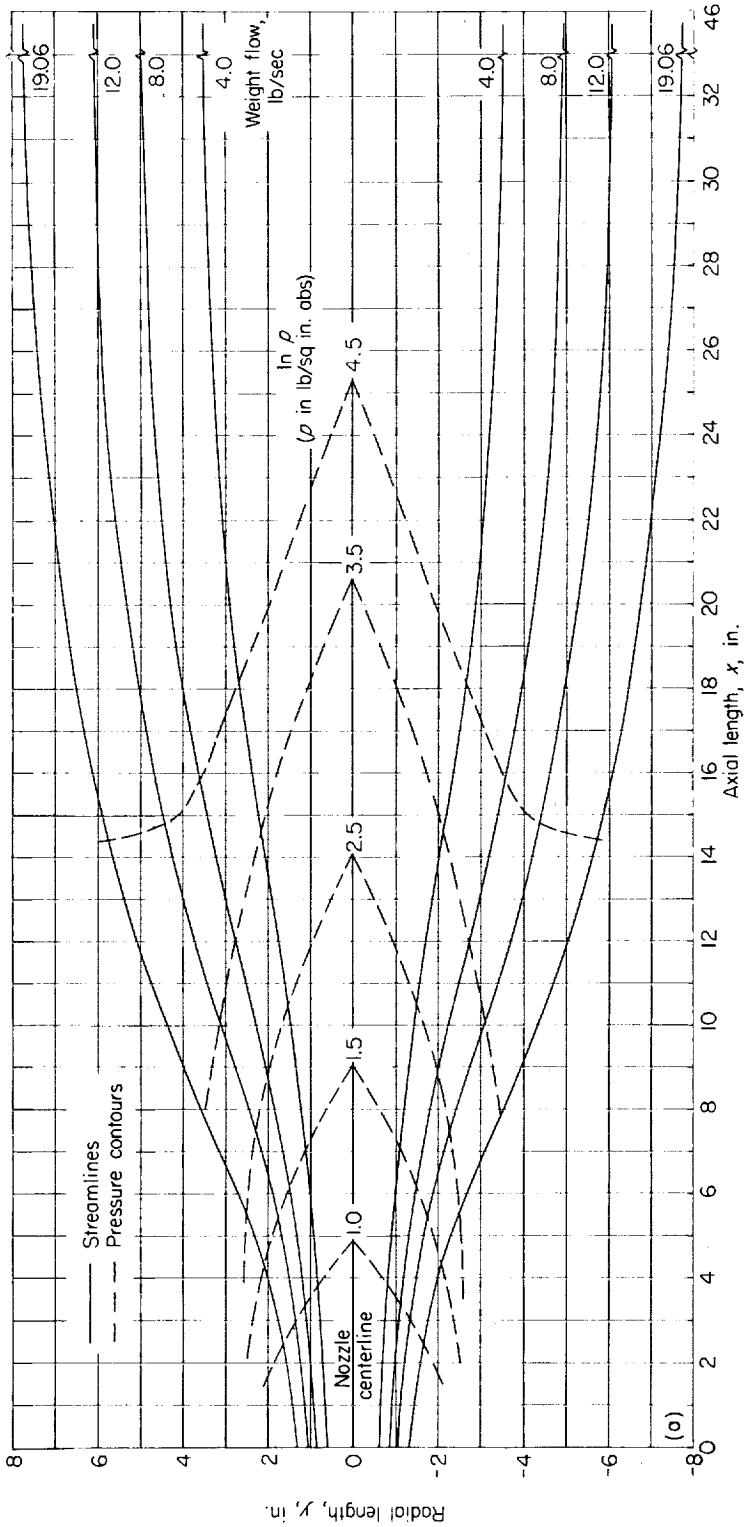

(a) Equilibrium composition (using variable γ).

FIGURE 6.—Streamlines and pressure contours for nozzles with a parabolic centerline pressure distribution.

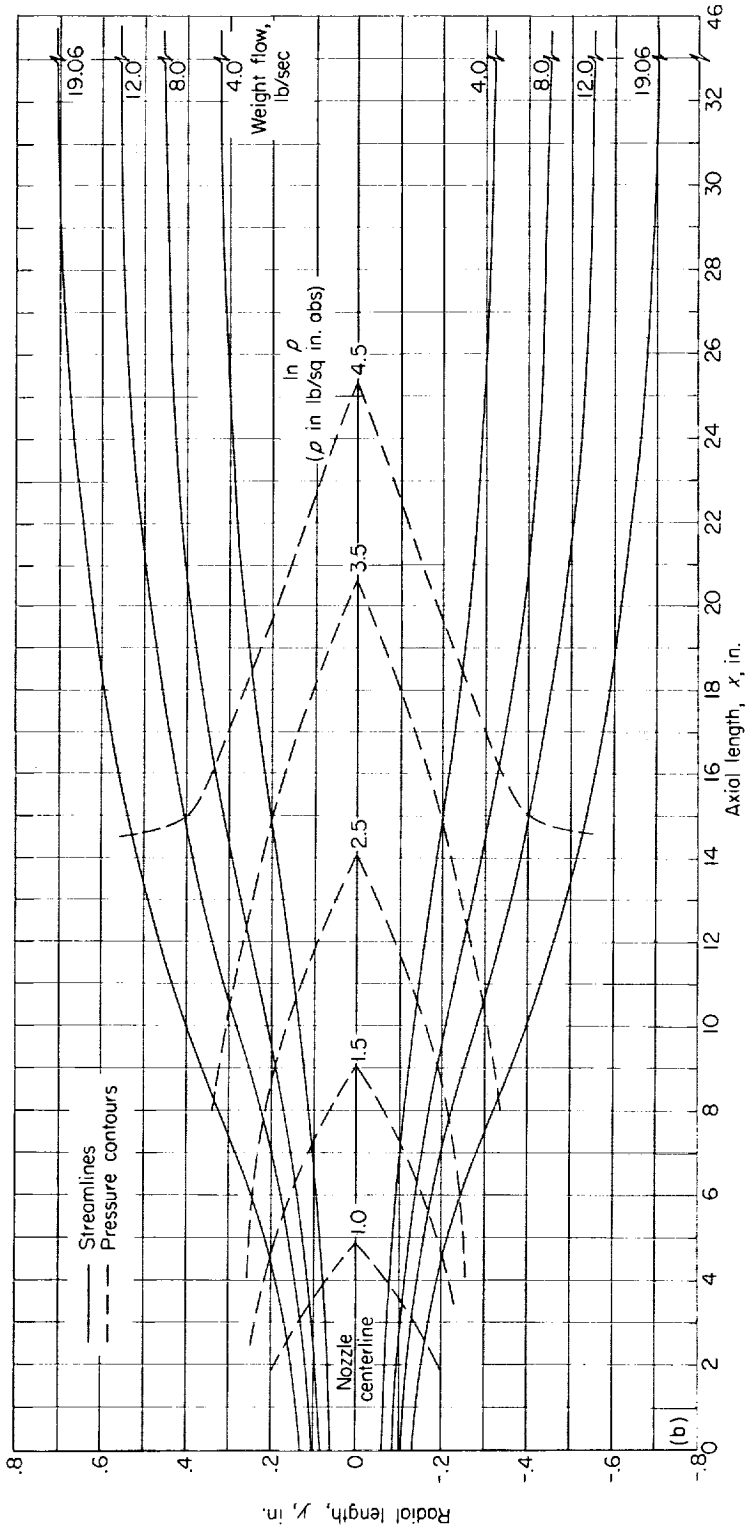

(b) Frozen composition (using variable γ).

FIGURE 6.—Continued. Streamlines and pressure contours for nozzles with a parabolic centerline pressure distribution.

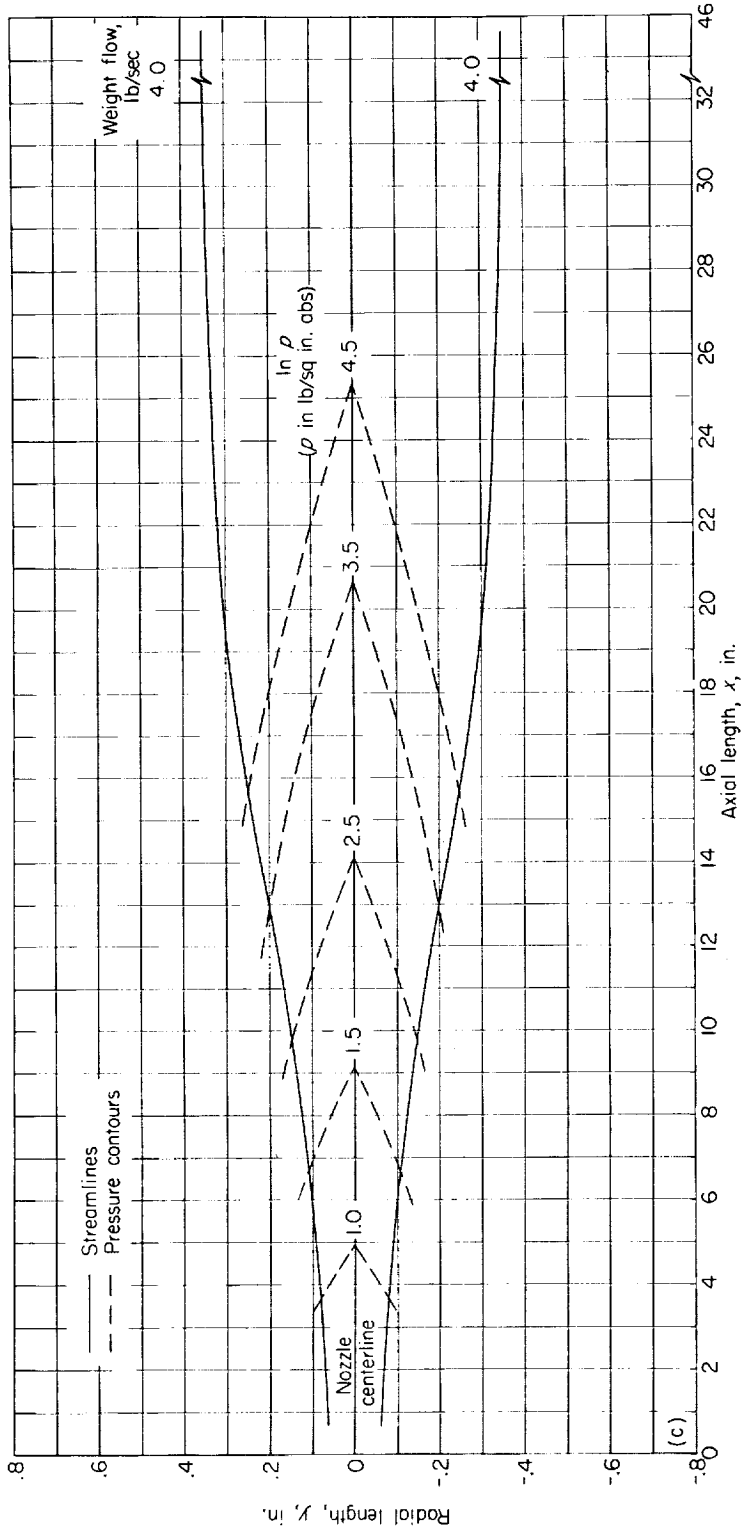

(c) Equilibrium composition (using constant γ).

FIGURE 6.—Continued. Streamlines and pressure contours for nozzles with a parabolic centerline pressure distribution.

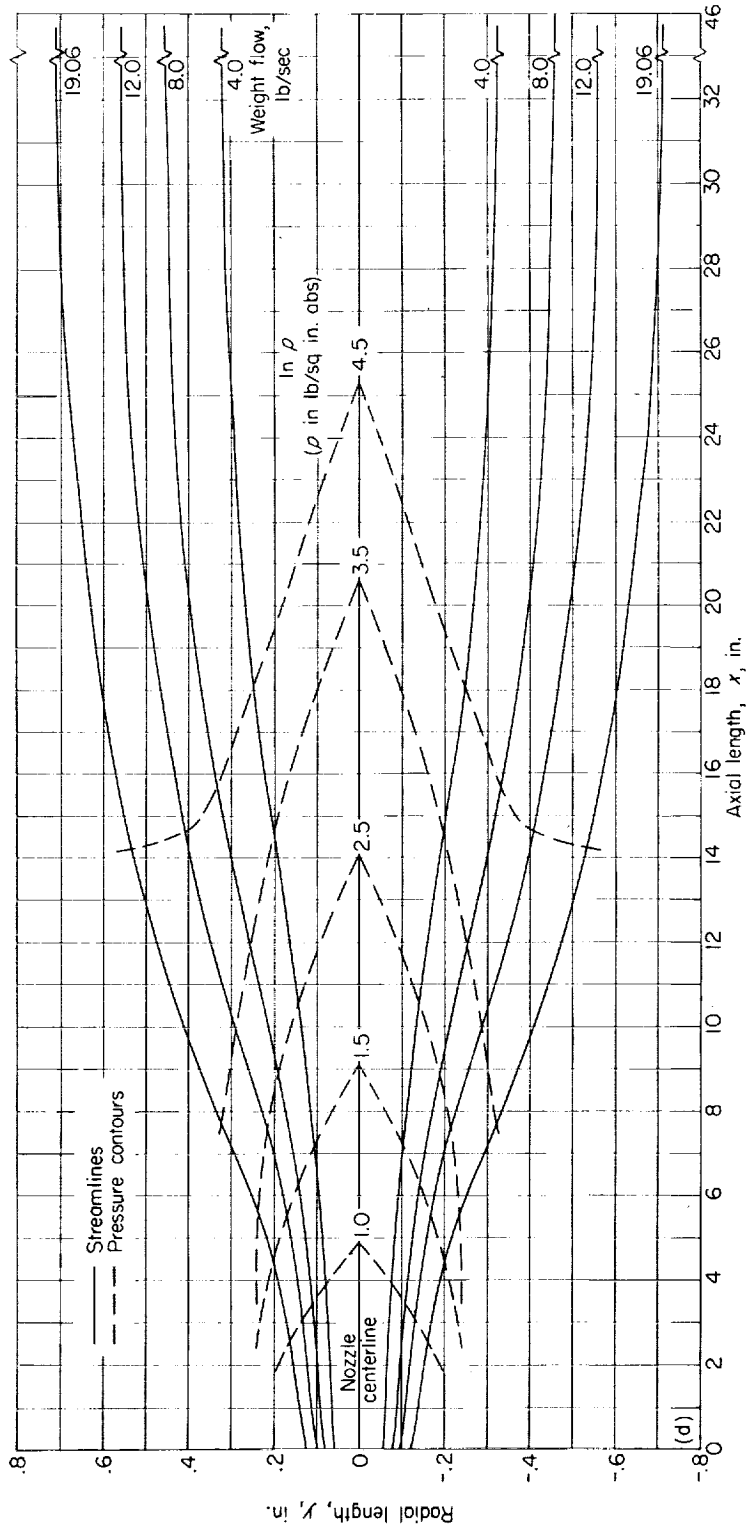

(d) Frozen composition (using constant γ).

FIGURE 6.—Concluded. Streamlines and pressure contours for nozzles with a parabolic centerline pressure distribution.

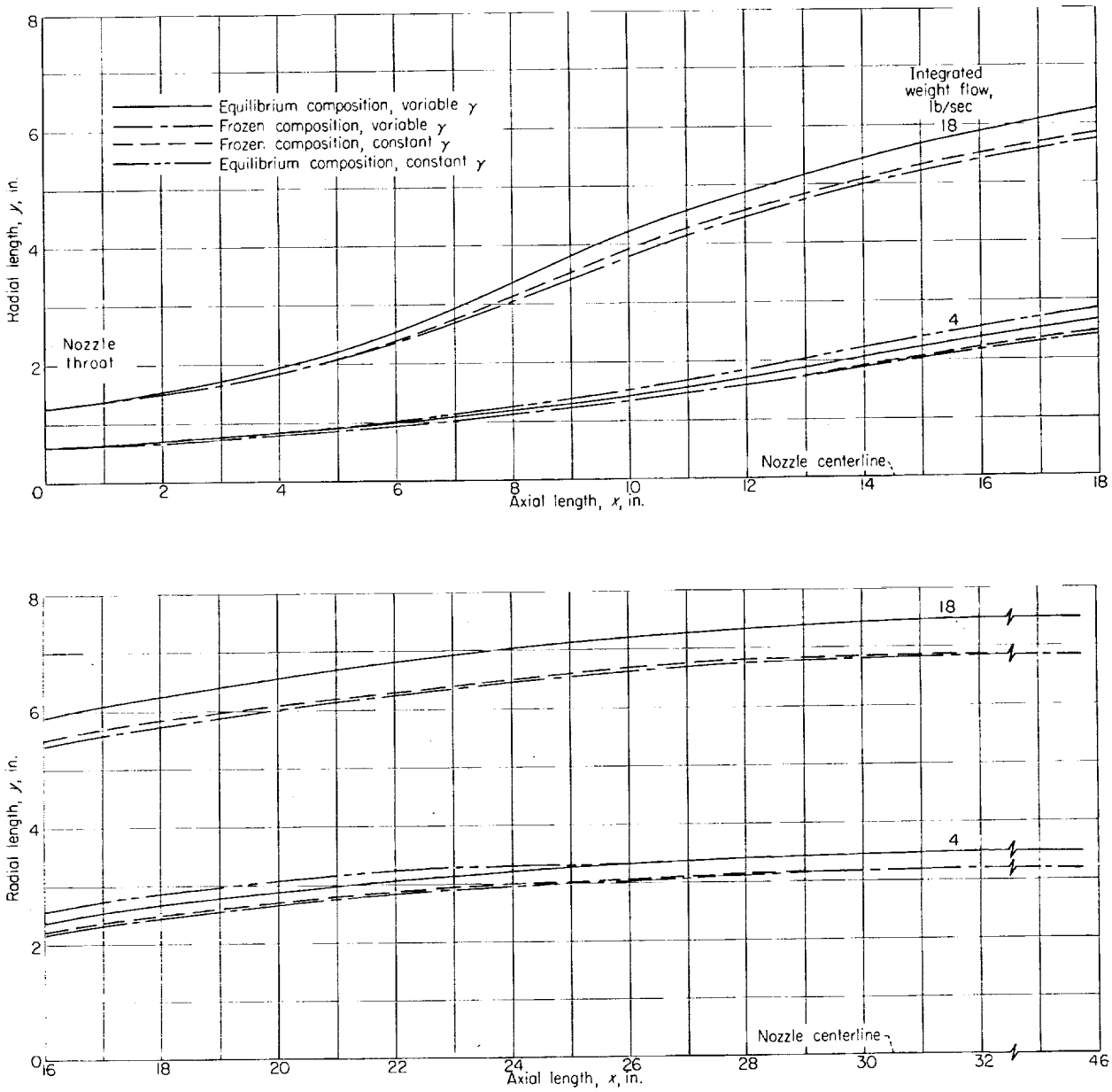

FIGURE 7.—Effect of frozen and equilibrium composition and isentropic exponent on nozzle contour for parabolic centerline pressure distribution and stoichiometric mixtures of ammonia and oxygen.

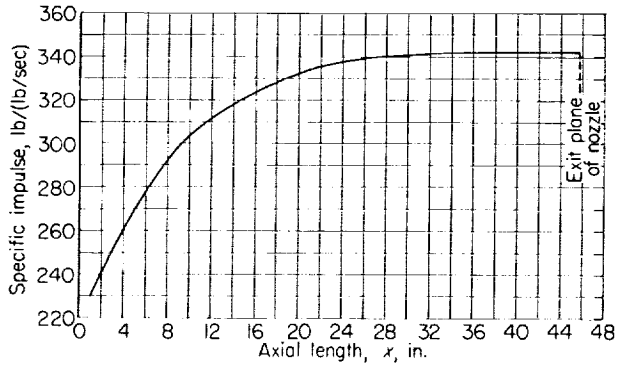

FIGURE 8.—Variation of vacuum specific impulse with axial length for a streamline. Weight flow, 4 pounds per second; equilibrium composition; constant isentropic exponent.

characteristic equations yielding short-length nozzles. Selection of adequate initial boundary conditions appears to be a trial-and-error process based upon previous experience. For the case where nozzle length is not important, designs are readily obtainable by utilizing a geometric scaling procedure. Several bell-shaped nozzles have been designed by specifying the initial boundary conditions along the nozzle centerline and by utilizing geometric scaling.

A comparison of nozzle contours obtained by assuming either frozen or equilibrium composition is presented. A comparison of contours for both compositions with either constant or variable isentropic exponent is also presented. Ammonia-oxygen was used as the propellant combination in the comparison. Significant differences among the contours of the examples indicated that the assumption of constant γ is inadequate and that actual thermodynamic data should be used in the solution of the characteristic flow equations.

A computation of the variation of vacuum specific impulse with axial length showed that considerable nozzle length, and hence weight, can be eliminated without serious thrust penalties in nozzle designs that gradually expand the flow to uniform exit conditions. For the example computed, a reduction in axial length of 50 percent resulted in only a 1.6-percent reduction in vacuum specific impulse.

LEWIS RESEARCH CENTER
NATIONAL AERONAUTICS AND SPACE ADMINISTRATION
CLEVELAND, OHIO, *February 11, 1959*

APPENDIX A

SYMBOLS

A,B,C,D,E	characteristic point identification
a	local speed of sound
c_p	specific heat at constant pressure
c_v	specific heat at constant volume
F	integrated thrust from centerline to point represented by subscript
f	arbitrary factor, eqs. (B1) and (B2)
g	acceleration of gravity
H	enthalpy
I	integrated specific impulse in vacuum from centerline to point represented by subscript
K_p,K_q	constant for conversion of units
$K_1,K_2,K_3,$ K_4,K_5,K_6	thermodynamic data curve-fitting coefficients, eq. (18)
L	characteristic line
$\mathscr{L}$	coefficient in characteristic equation
l	flow expansion length, axial distance along centerline for flow to expand from p_t to p_e, $l=$ (length of supersonic portion of nozzle) $-y_e/\tan\ \mu_e$
M	Mach number
$\mathscr{M}$	coefficient in characteristic equation
m	molecular weight
p	local static pressure
q	constant in eq. (21)
R	universal gas constant
T	local static temperature
t	tangent to characteristic line
u	component of velocity in x-direction
V	flow velocity
v	component of velocity in y-direction
w	integrated weight flow from centerline to point represented by subscript
x	axial distance along nozzle
y	radial dimension of nozzle
γ	isentropic exponent, $\gamma\equiv(\partial\ \ln\ p/\partial\ \ln\ \rho)_s$
θ	flow angle
μ	Mach angle, $\mu=\sin^{-1}1/M$
ρ	density
φ	enthalpy function

Subscripts:

A,B,C,D	characteristic point identification
c	chamber
e	exit
est	estimated
s	constant entropy
T	constant temperature
t	throat

Superscript:

$'$	second iteration

APPENDIX B

CALCULATION PROCEDURE

Unless extremely coarse grids are used, the number of equations and iterations involved in a nozzle characteristic network computation make hand-computational methods formidable. The method of characteristics applied to nozzle design as presented in this report therefore has been programmed and computed on an IBM 653 digital computer. Essentially the following procedure was employed in programming the method:

The calculation using the method of characteristics is initiated in the supersonic portion of the nozzle using an assumed pressure distribution along the centerline as the initial boundary conditions. The centerline static-pressure distribution is specified from the nozzle throat to the exit in terms of the natural logarithm of the static pressure as a function of the axial length along the nozzle centerline. The method of characteristics imposes no restriction on the centerline pressure distribution except that the function and at least the first derivative of the function should be continuous. Specification of a centerline pressure distribution will uniquely determine a flow field if a solution exists.

After the centerline pressure distribution is specified, grid points for the characteristic network are selected along the nozzle axis. A maximum grid spacing should be used; however, the spacing should also be fine enough to insure the accuracy desired in the finite-difference solution. A few trial grid spacings will determine the proper interval.

For convenience, the computation may be initiated at either the exit or the throat of the nozzle. The properties of the fluid at each of two adjacent points, D and E, along the nozzle axis may be determined from equations (14) to (18). Having a complete description of the flow along the nozzle axis, the characteristic equations can be solved to obtain the properties of the flow at the point C. As shown in figure 2, point C is defined by the intersection of the $\theta+\mu$ characteristics originating from point A and the $\theta-\mu$ characteristic originating from point B.

The determination of the flow properties at point C is an iterative process. The pressure and flow angle at C are initially estimated by any arbitrary scheme. The following relations were used to obtain the initial estimates:

$$\ln p_C = f(\ln p_A - \ln p_B) + \ln p_B \tag{B1}$$

and

$$\theta_C = (\theta_A - \theta_B)f + \theta_B \tag{B2}$$

where f is any arbitrary factor.

Based on the estimate of pressure and flow angle, a complete description of the flow properties at point C can be obtained from equations (14) to (18), inclusive.

The characteristic equations (7), (8), (11), and (12) can now be rewritten to provide first the location of the point C and then a check on the assumed values of flow angle and pressure. All coefficients in equations (7), (8), (11), and (12) are evaluated using properties that are the average of the estimated values at point C and the values at either point A or B. Thus, equations (7), (8), (11), and (12) become

$$x_C = \left\{ y_A - y_B + x_B \left[\frac{\tan(\theta_B - \mu_B) + \tan(\theta_{C,est} - \mu_{C,est})}{2} \right] - \left[\frac{\tan(\theta_A + \mu_A) + \tan(\theta_{C,est} + \mu_{C,est})}{2} \right] x_A \right\} \left[\frac{\tan(\theta_B - \mu_B) + \tan(\theta_{C,est} - \mu_{C,est})}{2} - \frac{\tan(\theta_A + \mu_A) + \tan(\theta_{C,est} + \mu_{C,est})}{2} \right]^{-1} \tag{B3}$$

$$y_C = y_A + (x_C - x_A) \left[\frac{\tan(\theta_A + \mu_A) + \tan(\theta_{C,est} + \mu_{C,est})}{2} \right] \tag{B4}$$

$$V_C=\frac{1}{4[(V_A+V_{C,est})^{-1}(\tan\mu_A+\tan\mu_{C,est})^{-1}+(V_B+V_{C,est})^{-1}(\tan\mu_B+\tan\mu_{C,est})^{-1}]}\left\{\frac{2}{\tan\mu_A+\tan\mu_{C,est}}\left[\frac{2V_A}{V_A+V_{C,est}}+\frac{\mathscr{L}_A+\mathscr{L}_{C,est}}{2}(x_C-x_A)\right]+\frac{2}{\tan\mu_B+\tan\mu_{C,est}}\left[\frac{2V_B}{V_B+V_{C,est}}+\frac{\mathscr{M}_B+\mathscr{M}_{C,est}}{2}(x_C-x_B)\right]+\theta_B-\theta_A\right\} \quad \text{(B5)}$$

and

$$\theta_C=\theta_A+\frac{2}{\tan\mu_A+\tan\mu_{C,est}}\left[\frac{2(V_C-V_A)}{V_{C,est}+V_A}-\frac{\mathscr{L}_A+\mathscr{L}_{C,est}}{2}(x_C-x_A)\right] \quad \text{(B6)}$$

Equation (B6) provides a direct check on the estimated value of flow angle. Equation (B5) provides the velocity at point C, which is an indirect check on the assumed static pressure. The flow angle from equation (B6) and the velocity from equation (B5) must agree with the assumed value of flow angle and the value of velocity obtained from equation (17) based on the assumed value of static pressure. Normally, the values of flow angle and velocity will not agree with the values initially assumed, and therefore additional iterations will be required to obtain convergence.

An estimate of the necessary change in the initial assumptions of flow angle and static pressure can be obtained by differentiating equation (17). Hence,

$$\frac{dV}{d\ln p}=\frac{-K_q^2}{2V}\frac{d\varphi}{d\ln p}=\frac{K_pT}{Vm} \quad \text{(B7)}$$

The static pressure and flow angle for the second and all additional iterations are then given by

$$\theta_{C'}=\theta_C+\Delta(\theta_C)/2 \quad \text{(B8)}$$

$$\ln p_{C'}=\ln p_C+\frac{V_C}{(T/m)_C K_p}\Delta(V_C) \quad \text{(B9)}$$

where ΔV_C and $\Delta\theta_C$ are the errors in the velocity and flow angle, respectively, in the previous iteration. This iteration procedure usually converged in three or four iterations.

The preceding procedure was carried out for each pair of adjacent points along the nozzle centerline. If there are n points specified along the nozzle axis, there will result $(n-1)$ points of C'. The calculation was then reinitiated using pairs of these $(n-1)$ points of C' as A and B points, and the process was repeated until the entire flow field of the nozzle was computed.

REFERENCES

1. Dillaway, Robert B.: A Philosophy for Improved Rocket Nozzle Design. Jet Prop., vol. 27, no. 10, Oct. 1957, pp. 1088–1093.
2. Graham, Robert W., Guentert, Eleanor Costilow, and Huff, Vearl N.: A Mach 4 Rocket-Powered Supersonic Tunnel Using Ammonia-Oxygen as Working Fluid. NACA TN 4325, 1958.
3. Ferri, Antonio: Elements of Aerodynamics of Supersonic Flows. The Macmillan Co., 1949.
4. Bridgman, P. W.: A Complete Collection of Thermodynamic Formulas. Phys. Rev., 2nd. ser., vol. III, no. 4, Apr. 1914, pp. 273–281.
5. Huff, Vearl N., Gordon, Sanford, and Morrell, Virginia E.: General Method and Thermodynamic Tables for Computation of Equilibrium Composition and Temperature of Chemical Reactions. NACA Rep. 1037, 1951. (Supersedes NACA TN's 2113 and 2161.)
6. Gordon, Sanford, and Wilkins, Roger L.: Theoretical Maximum Performance of Liquid Fluorine—Liquid Oxygen Mixtures with JP-4 Fuel as Rocket Propellants. NACA RM E54H09, 1954.
7. Gordon, Sanford, and Huff, Vearl N.: Theoretical Performance of Liquid Hydrazine and Liquid Fluorine as a Rocket Propellant. NACA RM E53E12, 1953.
8. Fortini, Anthony, and Huff, Vearl N.: Theoretical Performance of Liquid Hydrogen and Liquid Fluorine as a Rocket Propellant for a Chamber Pressure of 600 pounds per Square Inch Absolute. NACA RM E56L10a, 1957.
9. Huff, Vearl N., Fortini, Anthony, and Gordon, Sanford: Theoretical Performance of JP-4 Fuel and Liquid Oxygen as a Rocket Propellant. II – Equilibrium Composition. NACA RM E56D23, 1956.
10. Gordon, Sanford, and Glueck, Alan R.: Theoretical Performance of Liquid Ammonia with Liquid Oxygen as a Rocket Propellant. NACA RM E58A21, 1958.
11. Squires, R. K., Roberts, R. C., and Fisher, E. R.: A Method for Designing Supersonic Nozzles Using the Centerline Mach Number Distribution. NAVORD Rep. 3995, Naval Ord. Lab., Oct. 10, 1956.

U.S. GOVERNMENT PRINTING OFFICE: 1960